

Directional Materials—Nanoporous Organosilica Monoliths with Multiple Gradients Prepared Using Click Chemistry**

Andreas Schachtschneider, Martin Wessig, Martin Spitzbarth, Adrian Donner, Christian Fischer, Malte Drescher, and Sebastian Polarz*

Abstract: The existence of more than one functional entity is fundamental for materials, which are desired of fulfilling complementary or succeeding tasks. Whereas it is feasible to make materials with a homogeneous distribution of two different, functional groups, cases are extremely rare exhibiting a smooth transition from one property to the next along a defined distance. We present a new approach leading to high-surface area solids with functional gradients at the microstructural level. Periodically ordered mesoporous organosilicas (PMOs) and aerogel-like monolithic bodies with a maximum density of azide groups were prepared from a novel sol-gel precursor. The controlled and fast conversion of the azide into numerous functions by click chemistry is the prerequisite for the implementation of manifold gradient profiles. Herein we discuss materials with chemical, optical and structural gradients, which are interesting for all applications requiring directionality, for example, chromatography.

Biological matter has and still is setting important guiding principles for materials scientists.^[1] A key feature of almost any biological material is a hierarchical architecture,^[2] which is predominantly understood as a structural feature, respectively the organization of interrelated entities on successive length scales. A less noted, distinct element of hierarchy is the occurrence of specific gradients over changing dimensions. Consequently, materials scientists have thought about gradient materials as well, but the field stands quite at the beginning. In so-called functional gradient materials (FGMs),^[3] a sharp interface is replaced by a gradient at the microstructural level. This generates a smooth transition from one property to the next, and it is anticipated that this special character enables materials to perform more complex tasks. Despite the large interest in FGMs and their expected advanced properties, there exist only limited examples. Still the vast majority of functional materials presented nowadays


in current literature contains phases, which have to be described as homogeneous in nature, lacking any gradient. Homogeneity is regarded rather as a criterion of quality.

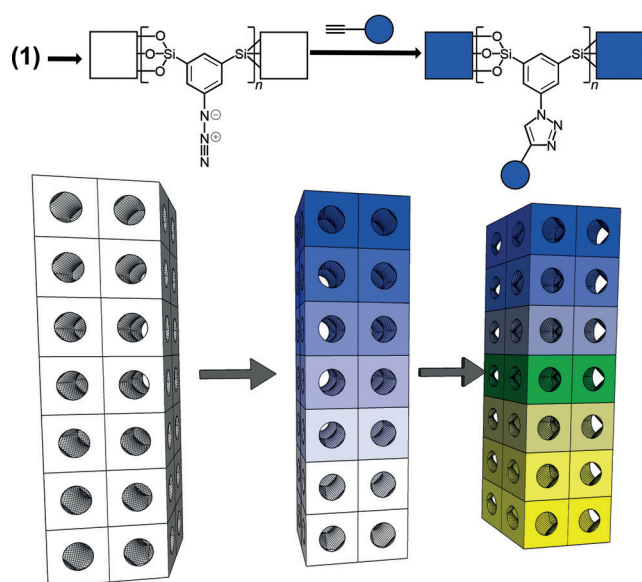
One can roughly divide FGMs into two categories: Either the gradient comprises the bulk-phase of the material, or one finds a gradient on a surface. The first functional (bulk-phase) gradient materials found in literature date back to 1978, when the optical properties of lenses made from materials with successive refractive indices were studied.^[4] Several other examples followed.^[3,5] A very recent example was presented by Sun et al. addressing the role of a concentration gradient in Li-ion battery solids.^[5g] It took much longer until materials with surface chemical gradients could be realized, and the number of known examples is much smaller. In an important contribution the surfaces of a silicon wafer was modified using decyltrichlorosilane.^[6] A gradient in hydrophobic character resulted from locally different surface coverage, and this induced water droplets to run uphill. The system was studied in detail and the principle was adopted and transferred to other materials.^[7] The latter examples indicate that the preparation of gradient surfaces represents a difficult but valuable task. However, it would be highly interesting to provide gradient materials with much higher specific surface area than a plane substrate, and it could be promising to combine this with a much richer variability of functional groups compared to the discussed “hydrophobic–hydrophilic theme”. We aim at establishing the concept of functional gradient materials in the field of nanoporous organosilica materials. Ultimately, orthogonal gradients of different groups should be generated (see Scheme 1).

The advantage of nanoporous materials is, that they provide a large internal surface area, and substantial knowledge exists about their preparation.^[8] Methods for chemical surface modification of SiO₂ materials are highly developed.^[9] Amongst the different organosilica materials, the so-called bridged polysilsesquioxane materials (BPSOs) prepared from special sol-gel precursors X₃Si-R-SiX₃ (where R is a bridging organic group and X is a hydrolysable group) are of extraordinary importance.^[10] Using structure directing agents the so-called PMOs (periodically ordered mesoporous organosilica materials) with uniform pore systems have been established.^[11] A key advantage of using BPSOs is that materials can be prepared without diluting the precursors entity, and this results in a maximum regarding the degree of organic modification.^[12] The distribution of the functional organic groups is homogeneous throughout the entire material, and yet the number of examples for bifunctional materials is small.^[13] Considering the high stage of development in nanoporous materials research, it is also astonishing

[*] A. Schachtschneider, M. Wessig, M. Spitzbarth, A. Donner, C. Fischer, Dr. M. Drescher, Prof. Dr. S. Polarz
Department of Chemistry, University of Konstanz
Universitätsstrasse 10
E-mail: sebastian.polarz@uni-konstanz.de
Homepage: <http://cms.uni-konstanz.de/polarz/>

[**] We thank the German Research Foundation (Deutsche Forschungsgemeinschaft, DFG) for funding within the SPP 1570 (PO 780/14-1). Further financial support by the DFG (DR 743/7-1). We thank Prof. M. Tiemann (Paderborn) and Micromeritics for Hg porosimetry measurements.

 Supporting information for this article, including experimental details, is available on the WWW under <http://dx.doi.org/10.1002/anie.201502878>.



Scheme 1. Preparation of nanoporous organosilica materials containing functional surface gradients (for the synthesis of **1** see the Supporting Information). Using the phenylazide BPSO (white), one can introduce a multitude of functional groups (blue) by 1,3-dipolar Huisgen cycloaddition. Ultimately, a second gradient of a different functional group (yellow) can be generated.

that there is almost nothing known about nanoporous gradient materials. Mesoporous organosilica materials with chemical gradients of two different functional groups do not exist to the best of our knowledge.

For realizing the latter goal, we intend to prepare nanoporous organosilica materials containing organic groups imbedded in the pore surfaces, which can be transferred as easy as possible, rapidly and reproducibly into a large variety of functional groups. Then, we will explore methods for generating different chemical gradients (see Scheme 1). When one is looking for a chemical system of enormous versatility and high tolerance against numerous functional groups, one inevitably finds click reactions, and in particular the 1,3-dipolar Huisgen cycloaddition (Scheme 1).^[14] Huesing and Keppeler could modify mesoporous SiO₂ with azide groups by post-modification and showed the general feasibility of click chemistry in pores.^[15] An alternative approach for post-modification of materials by click chemistry is the use of the thiol-ene reaction, which was for instance nicely demonstrated by the research group of Van Der Voort and co-workers.^[16] A comprehensive review about click chemistry in materials science was published very recently by Bowman and co-workers,^[17] and interestingly no FGMs were mentioned.^[18]

1,3-Bis-tri-isopropoxysilyl-phenyl-5-azide (**1**) can be identified as a required, new sol-gel precursor (Scheme 1). Because N₃[−] can be regarded as a so-called pseudo-halogenide ion,^[19] the exchange of Br[−] with N₃[−] can be achieved easily by adopting a literature procedure^[20] with 1,3-bis-tri-isopropoxysilyl-phenyl-5-bromide as a starting compound (see the Experimental Section in the Supporting Information and Supporting Information S-1).^[21] The substitution works quan-

titatively, and the molecular precursor compound was characterized unambiguously (see also the Supporting Information S-1). The main signal ($m/z = 529.3 \text{ g mol}^{-1}$) observed in electron spray ionization mass spectrometry (ESI-MS) fits precisely to the protonated form of (**1**). In the ¹⁵N-NMR spectrum one sees three signals at $\delta = -138$, -149 and -283 ppm , which fit well to phenyl azide as a related compound,^[22] and demonstrates the purity of the compound.

As a BPSO precursor, one should be able to use (**1**) for the preparation of PMO materials. True liquid crystal templating^[23] was achieved using an amphiphilic blockcopolymer as a structure directing agent present. The small angle X-ray scattering (SAXS) pattern of the obtained material shown in Figure 1a contains a series of signals with d-spacing in ratios

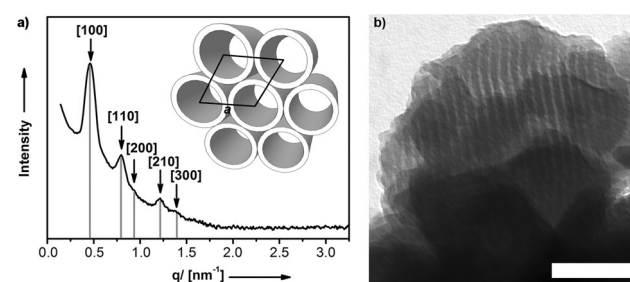


Figure 1. a) SAXS pattern and b) TEM micrograph (scale bar = 100 nm) of the novel PMO material containing phenylazide.

of $1:1/\sqrt{3}:1/\sqrt{4}:1/\sqrt{7}$, which is typical for the columnar hexagonal mesophase with $p6mm$ symmetry. Evaluation using the program package SCATTER^[24] yields a value of 15.7 nm for the lattice constant a . The investigation of the material using TEM (Figure 1b) and physisorption analysis (S-2) shows that a mesoporous material with an average pore size of 6.7 nm and a specific surface area of $445 \text{ m}^2 \text{ g}^{-1}$ could be obtained. Because the adsorbed volume at $p/p^0 = 0.08$ is one third of the total adsorbed volume, it can be expected that the pore walls contain a substantial amount of micropores.^[25]

It is worth noting that BPSO precursors are almost exclusively used for the synthesis of PMOs, and much less is known about the generation of alternative porous structures like aerogels.^[26] A particular difficulty is the preparation of monolithic bodies.^[27] The use of precursor (**1**) for making aerogel-type monoliths was demanding, also because unlike to typical sol-gel processes a one-step procedure was not successful. Basic pH values are not suitable because the bulky isopropoxy-groups prohibit sufficient hydrolysis rates. Even after about one week no hydrolysis of the SiO^{iso}Pr groups could be observed at all (see section S-3). Low pH-values (< 1) are required, but at such conditions polycondensation and gelation is of the order of weeks. Therefore, a two-step procedure was developed, and macroscopic gel bodies could be prepared within 2 days. After supercritical drying, highly porous aerogel monoliths (Figure 2a) could be obtained (see also S-4). The porosity of such aerogels can be as high as 92 %, and the specific surface area was $662 \text{ m}^2 \text{ g}^{-1}$. Investigation using scanning electron microscopy (SEM) and TEM shows the typical, fractal nature of the porous network. Despite the

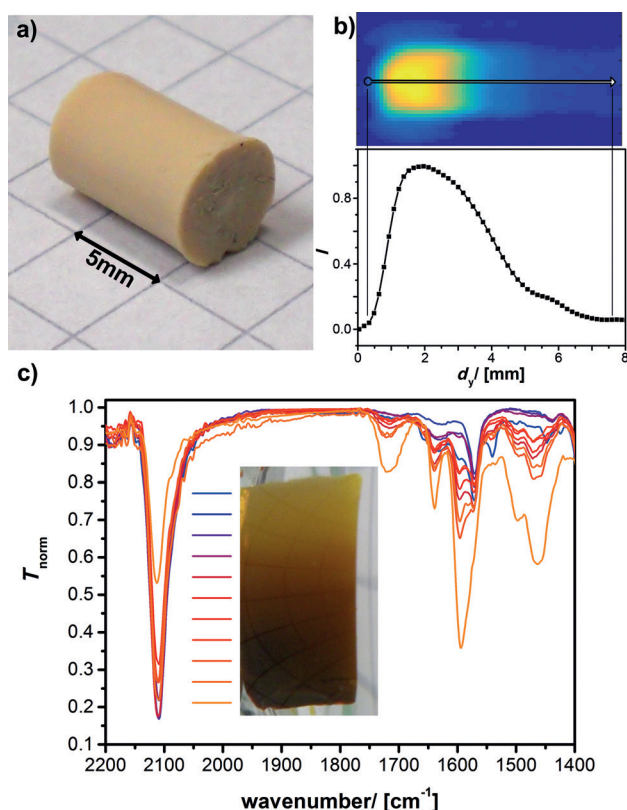


Figure 2. a) Dry monolith of the nanoporous phenylazide organosilica material, b) EPR mapping of the distribution of TEMPO attached to the azide groups by click chemistry, and c) photographic image of a monolith characterized by a gradient in surface-attached fluoresceine and IR spectra taken from different positions.

high porosity, the monoliths show a sufficient mechanical stability to be handled without great care. The force/pressure, which can be applied to the monolith until it breaks, was determined and is 3.5 N cm^{-2} .

The chemical fingerprint of all prepared, porous materials (PMO materials and aerogels) was obtained from solid-state NMR spectroscopy, thermogravimetric analysis (TGA) and FT-IR spectroscopy and is exemplarily given in section S-5. The chemical shift of the ^{13}C NMR signals fits very well to those from the precursor. In FT-IR one can clearly identify the characteristic vibrations for the azide group ($\nu_{\text{asym}} = 2100 \text{ cm}^{-1}$; $\nu_{\text{sym}} = 1284 \text{ cm}^{-1}$). A mass loss step ($\Delta m = -12\%$) is observed at $T = 188^\circ\text{C}$, which can be assigned to the loss of one nitrogen molecule from the organosilica material. Because also using ^{29}Si -NMR one cannot see any cleavage of the Si-C bond, one can assign the desired composition $\text{Si}_2\text{O}_3\text{C}_6\text{H}_3\text{N}_3$ to the obtained materials.

There are two obvious variants for utilizing the azide entity for click derivatization. One possibility is the reaction with the sol-gel precursor (**1**) on the molecular scale, and its feasibility could be proven by NMR spectroscopy (see S-6). However, because the latter approach would yield materials with a homogeneous distribution of functional groups, for achieving gradient materials we investigated if the click reaction could be done in the solid state, too (Scheme 1). In the following, only monolithic aerogel materials are dis-

cussed. Due to good spectroscopic visibility ethyl propiolate (see S-7a) was used for the first steps. The success of the click reaction can be demonstrated by ^{13}C NMR (data shown in S-8). Additional ^{13}C NMR signals appear at $\delta = 211$ (C=O), 152 (triazol C-R) and 113 ppm (triazol C-H). In FTIR one sees that $\nu_{\text{asym}}(\text{N}_3)$ vanishes whereas a band at 1728 cm^{-1} characteristic for C=O in propiolate appears (see Figure 3).

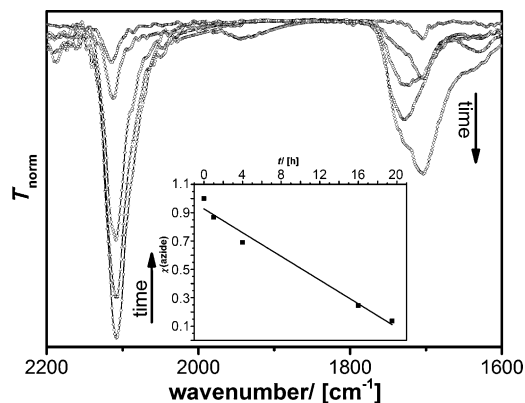


Figure 3. Time-dependent FTIR for the click reaction with ethyl propiolate. The inset shows the fraction of non-reacted azide as a function of time.

Monitoring the rate of conversion shows that there is an almost linear dependency, which means that the degree of derivatization can be adjusted precisely with time. Up to 87% of the azide groups can be converted, which is a fairly high value. At the same time, the monolithic character and the high porosity of the material remain intact as indicated by physisorption measurements (see S-8c for the ethyl-propiolate derivatization). It should also be emphasized that other, more functional groups can be introduced whenever a suitable alkyne is accessible (S-7). A material with superhydrophobic character obtained by modification with a fluorinated phenyl entity (see S-7c) is given as an example in the Supporting Information (see S-9).

Up to this point, the entire monolithic body was exposed to the solution containing the ingredients for the click reaction resulting in a homogeneous modification. Achieving a gradient is imaginably simple. One dips only one side of the monolith into the solution as shown in S-10. By adjusting the amount of the alkyne reagent this automatically leads to the formation of a distribution profile, and also other parameters like contact time, solvent properties, temperature can influence the result. The success of our method can be monitored directly by imaging techniques, for instance electron paramagnetic spectroscopy (EPR) imaging.^[28] For this purpose 4-ethynoxy-2,2,6,6-tetramethylpiperidin-1-oxyl (see S-7e), an alkyne, containing a persistent TEMPO nitroxide radical derivative, was synthesized and used for the click reaction.^[29] The EPR spectrum of the attached TEMPO derivative shown in S-11 is characteristic for a probe with an anisotropic and reduced rotation caused by the successful attachment to the surface. The spectroscopic information was used for EPR imaging analysis for separation of the spatial information by

performing a deconvolution prior to image reconstruction using filtered back projection.^[30] The intensity of the spatially resolved signal is proportional to the local density of TEMPO, the created, and the chemical gradient can be seen (Figure 2b). There is large freedom regarding the geometric extension of the gradient, as shown for a different monolith in S-12. Currently, the gradient can be controlled on the scale of millimeters up to centimetres.

To show the creation of chemical gradients for an independent system, we have also prepared alkyne-modified dyes like fluoresceine (FI; see also S-7g). Figure 2c shows a photographic image of a porous organosilica monolith characterized by a FI gradient, additionally proven by spatially resolved IR spectra. One sees the gradual decrease of the azide modes accompanied by an increase in bands corresponding to FI, when one is moving from top to bottom of the monolith. A second group can be introduced by turning the monolith and dipping it into a click solution containing a second functionality (e.g. rhodamine B (RhB); S-7f), resulting in a material with double-gradient character (for a photographic image see S-11). As expected, at the top of such a bigradient material one can only observe the optical features of FI ($\lambda_{\text{max,ex}}(\text{FI}) = 499 \text{ nm}$; $\lambda_{\text{max,em}}(\text{FI}) = 554 \text{ nm}$) and at the bottom those of RhB ($\lambda_{\text{max,ex}}(\text{RhB}) = 560 \text{ nm}$; $\lambda_{\text{max,em}}(\text{RhB}) = 624 \text{ nm}$) as shown in Figure 4a,c. However, in the

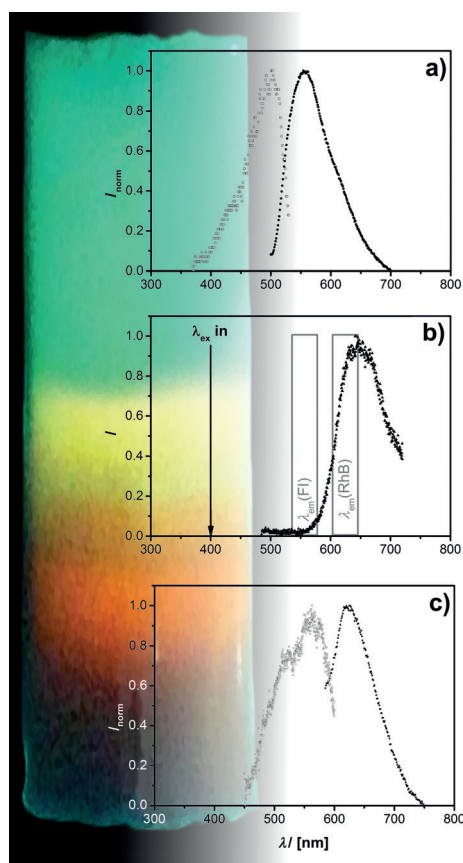


Figure 4. Fluorescence image ($\lambda_{\text{exc}} = 400 \text{ nm}$) of a FI (top \rightarrow bottom)/RhB (bottom \rightarrow top) bi-gradient monolith (length of the monolith: 1.2 cm) and PL spectra taken from different positions. Excitation (hollow symbols) and emission (solid symbols).

middle region a new, emergent feature is found (Figure 4b). Although a wavelength $\lambda = 400 \text{ nm}$ is not suitable for the excitation of RhB, exclusively its fluorescence signal can be detected. This phenomenon can be explained by Foerster resonance energy transfer (FRET).^[31] When the two dyes are present in a proper ratio and are close enough to each other, as is obviously the case in middle region of the monolith, excited FI may transfer its energy to RhB, which then exhibits fluorescence.

The gradient functionalization of the porous organosilica materials grants to explore another highly interesting possibility: The creation of materials with structural gradients, for example, a gradient in pore-size. The network of the as-prepared phenylazide material can be densified by treatment with polar solvents. We found that the extent of these processes correlate to the degree of azide derivatization with hydrophobic groups, for example, with phenylacetylene. Treating a material characterized by a gradient of phenylacetylene leads to a new gradient due to the locally varying magnitude of polycondensation and associated shrinkage (see Figure 5). The extent of shrinkage directly influences the

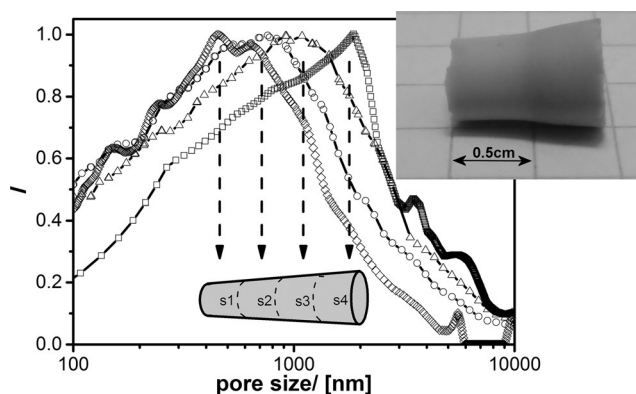


Figure 5. Pore-size distribution functions (obtained from mercury intrusion porosimetry) for different segments (s) along a gradient organosilica monolith also shown as a photographic image.

average pore size of the aerogel. For analytical proof, the monolith was cut into different parts, and each part was analysed by mercury intrusion porosimetry (see also S-14). One sees that the maximum of the resulting pore-size distribution functions (Figure 5) is shifting gradually from larger values (for the less shrunk regions) to lower values. Please also note, that due to the logarithmic scale on the x-axis the actual shift of the pore-size ($D_{\text{max}}(s1) = 457 \text{ nm} \rightarrow D_{\text{max}}(s2) = 1872 \text{ nm}$) is pronounced. Furthermore, segments with a substantial width (see Figure 5a) were needed for having sufficient material for a measurement. Therefore, the pore-size distribution function is expected to be narrower for infinitesimal segments than actually shown in Figure 5. It should be noted that due to the fragile nature of aerogels and the high pressure applied during Hg porosimetry, it cannot be excluded that (partial) changes in the materials occur.^[32] Because our findings are also in agreement with SEM data (see S-14), one can state that the pore-size gradient is of the order of 1000 nm per 1 cm extension of the monolith.

Herein we have demonstrated that the use of a new sol-gel precursor of the PMO-type comprising a bridging phenylazide entity leads to a variety of unique possibilities. Not only PMOs but also monolithic bodies of aerogel-like materials could be prepared. Almost any desired functional group can be attached using click chemistry. Furthermore, it was possible to create nanoporous solids with either chemical or structural gradients, which will make the materials promising for a range of applications, for example, in chromatography or catalysis.

Keywords: click chemistry · gradients · hybrid materials · nanoporous materials · surface modification

How to cite: *Angew. Chem. Int. Ed.* **2015**, *54*, 10465–10469
Angew. Chem. **2015**, *127*, 10611–10615

- [1] a) S. Mann, G. A. Ozin, *Nature* **1996**, *382*, 313–318; b) S. Mann, *Nature* **1993**, *365*, 499–505; c) H. J. Gao, B. H. Ji, I. L. Jager, E. Arzt, P. Fratzl, *Proc. Natl. Acad. Sci. USA* **2003**, *100*, 5597–5600; d) M. A. Meyers, P. Y. Chen, A. Y. M. Lin, Y. Seki, *Prog. Mater. Sci.* **2008**, *53*, 1–206.
- [2] P. Fratzl, R. Weinkamer, *Prog. Mater. Sci.* **2007**, *52*, 1263–1334.
- [3] B. H. Rabin, I. Shiota, *MRS Bull.* **1995**, *20*, 14–18.
- [4] D. T. Moore, D. P. Ryan, *J. Opt. Soc. Am.* **1978**, *68*, 1157–1166.
- [5] a) C. C. M. Wu, M. Kahn, W. Moy, *J. Am. Ceram. Soc.* **1996**, *79*, 809–812; b) A. Neubrand, J. Rodel, *Z. Metallk.* **1997**, *88*, 358–371; c) A. Neubrand, *J. Appl. Electrochem.* **1998**, *28*, 1179–1188; d) Y. Einaga, G. S. Kim, K. Ohnishi, S. G. Park, A. Fujishima, *Mater. Sci. Eng. B* **2001**, *83*, 19–23; e) S. T. Plummer, P. W. Bohn, *Langmuir* **2002**, *18*, 4142–4149; f) T. Sehayek, A. Vaskevich, I. Rubinstein, *J. Am. Chem. Soc.* **2003**, *125*, 4718–4719; g) Y. K. Sun, D. H. Kim, C. S. Yoon, S. T. Myung, J. Prakash, K. Amine, *Adv. Funct. Mater.* **2010**, *20*, 485–491.
- [6] M. K. Chaudhury, G. M. Whitesides, *Science* **1992**, *256*, 1539–1541.
- [7] a) B. Liedberg, P. Tengvall, *Langmuir* **1995**, *11*, 3821–3827; b) B. J. Jeong, J. H. Lee, H. B. Lee, *J. Colloid Interface Sci.* **1996**, *178*, 757–763; c) R. H. Terrill, K. M. Balss, Y. M. Zhang, P. W. Bohn, *J. Am. Chem. Soc.* **2000**, *122*, 988–989; d) S. Daniel, M. K. Chaudhury, J. C. Chen, *Science* **2001**, *291*, 633–636; e) R. R. Fuierer, R. L. Carroll, D. L. Feldheim, C. B. Gorman, *Adv. Mater.* **2002**, *14*, 154; f) J. L. Zhang, L. J. Xue, Y. C. Han, *Langmuir* **2005**, *21*, 5–8; g) X. Yu, Z. Q. Wang, Y. G. Jiang, X. Zhang, *Langmuir* **2006**, *22*, 4483–4486.
- [8] S. Polarz, B. Smarsly, *J. Nanosci. Nanotechnol.* **2002**, *2*, 581–612.
- [9] a) F. Hoffmann, M. Cornelius, J. Morell, M. Froba, *Angew. Chem. Int. Ed.* **2006**, *45*, 3216–3251; *Angew. Chem.* **2006**, *118*, 3290–3328; b) L. Nicole, C. Boissiere, D. Grosso, A. Quach, C. Sanchez, *J. Mater. Chem.* **2005**, *15*, 3598–3627; c) R. Wu, L. G. Hu, F. J. Wang, M. L. Ye, H. Zou, *J. Chromatogr. A* **2008**, *1184*, 369–392; d) A. Vinu, K. Z. Hossain, K. Ariga, *J. Nanosci. Nanotechnol.* **2005**, *5*, 347–371; e) T. Yokoi, H. Yoshitake, T. Tatsumi, *J. Mater. Chem.* **2004**, *14*, 951–957; f) S. Huh, J. W. Wiench, J. C. Yoo, M. Pruski, V. S. Y. Lin, *Chem. Mater.* **2003**, *15*, 4247–4256.
- [10] a) K. J. Shea, D. A. Loy, *Chem. Mater.* **2001**, *13*, 3306–3319; b) A. P. Wight, M. E. Davis, *Chem. Rev.* **2002**, *102*, 3589–3613.
- [11] a) B. Hatton, K. Landskron, W. Whitnall, D. Perovic, G. A. Ozin, *Acc. Chem. Res.* **2005**, *38*, 305–312; b) P. Van der Voort, D. Esquivel, E. De Canck, F. Goethals, I. Van Driessche, F. J. Romero-Salguero, *Chem. Soc. Rev.* **2013**, *42*, 3913–3955.
- [12] K. Landskron, B. D. Hatton, D. D. Perovic, G. A. Ozin, *Science* **2003**, *302*, 266–269.
- [13] a) T. Asefa, M. Kruk, M. J. MacLachlan, N. Coombs, H. Grondey, M. Jaroniec, G. A. Ozin, *J. Am. Chem. Soc.* **2001**, *123*, 8520–8530; b) J. Alauzun, A. Mehdi, C. Reye, R. J. P. Corriu, *J. Am. Chem. Soc.* **2006**, *128*, 8718–8719; c) K. K. Sharma, T. Asefa, *Angew. Chem. Int. Ed.* **2007**, *46*, 2879–2882; *Angew. Chem.* **2007**, *119*, 2937–2940; d) A. Kuschel, M. Drescher, T. Kuschel, S. Polarz, *Chem. Mater.* **2010**, *22*, 1472–1482; e) A. Kuschel, S. Polarz, *J. Am. Chem. Soc.* **2010**, *132*, 6558–6565.
- [14] H. C. Kolb, M. G. Finn, K. B. Sharpless, *Angew. Chem. Int. Ed.* **2001**, *40*, 2004; *Angew. Chem.* **2001**, *113*, 2056–2075.
- [15] M. Keppeler, N. Husing, *New J. Chem.* **2011**, *35*, 681–690.
- [16] a) D. Esquivel, O. van den Berg, F. J. Romero-Salguero, F. Du Prez, P. Van Der Voort, *Chem. Commun.* **2013**, *49*, 2344–2346; b) M. Ide, E. De Canck, I. Van Driessche, F. Lynen, P. Van Der Voort, *RSC Adv.* **2015**, *5*, 5546–5552.
- [17] W. Xi, T. F. Scott, C. J. Kloxin, C. N. Bowman, *Adv. Funct. Mater.* **2014**, *24*, 2572–2590.
- [18] a) J. Nakazawa, T. D. P. Stack, *J. Am. Chem. Soc.* **2008**, *130*, 14360; b) A. Schlossbauer, D. Schaffert, J. Kecht, E. Wagner, T. Bein, *J. Am. Chem. Soc.* **2008**, *130*, 12558–0; c) A. Schlossbauer, S. Warncke, P. M. E. Gramlich, J. Kecht, A. Manetto, T. Carell, T. Bein, *Angew. Chem. Int. Ed.* **2010**, *49*, 4734–4737; *Angew. Chem.* **2010**, *122*, 4842–4845; d) C. H. Chu, R. H. Liu, *Chem. Soc. Rev.* **2011**, *40*, 2177–2188.
- [19] a) A. Schulz, A. Villinger, *Chem. Eur. J.* **2010**, *16*, 7276–7281; b) H. Brand, A. Schulz, A. Villinger, *Z. Anorg. Allg. Chem.* **2007**, *633*, 22–35.
- [20] J. Andersen, U. Madsen, F. Bjorkling, X. F. Liang, *Synlett* **2005**, 2209–2213.
- [21] A. Kuschel, S. Polarz, *Adv. Funct. Mater.* **2008**, *18*, 1272–1280.
- [22] J. Müller, *Z. Naturforsch. B* **1979**, *34*, 437–441.
- [23] a) B. Smarsly, M. Antonietti, *Eur. J. Inorg. Chem.* **2006**, 1111–1119; b) S. Polarz, M. Antonietti, *Chem. Commun.* **2002**, 2593–2604.
- [24] a) S. Förster, A. Timmann, M. Konrad, C. Schellbach, A. Meyer, S. S. Funari, P. Mulvaney, R. Knott, *J. Phys. Chem. B* **2005**, *109*, 1347–1360; b) S. Förster, L. Apostol, W. Bras, *J. Appl. Crystallogr.* **2010**, *43*, 639–646; c) S. Förster, C. Burger, *Macromolecules* **1998**, *31*, 879–891.
- [25] C. G. Göltner, B. Smarsly, B. Berton, M. Antonietti, *Chem. Mater.* **2001**, *13*, 1617–1624.
- [26] a) A. C. Pierre, G. M. Pajonk, *Chem. Rev.* **2002**, *102*, 4243–4265; b) N. Hüsing, U. Schubert, *Angew. Chem. Int. Ed.* **1998**, *37*, 22–45; *Angew. Chem.* **1998**, *110*, 22–47.
- [27] D. Brandhuber, V. Torma, C. Raab, H. Peterlik, A. Kulak, N. Husing, *Chem. Mater.* **2005**, *17*, 4262–4271.
- [28] a) D. A. Cleary, Y. K. Shin, D. J. Schneider, J. H. Freed, *J. Magn. Reson.* **1988**, *79*, 474–492; b) Y. K. Shin, U. Ewert, D. E. Budil, J. H. Freed, *Biophys. J.* **1991**, *59*, 950–957; c) O. E. Yakimchenko, E. N. Degtyarev, V. N. Parmon, Y. S. Lebedev, *J. Phys. Chem.* **1995**, *99*, 2038–2041; d) A. Marek, J. Labsky, C. Konak, J. Pilar, S. Schlick, *Macromolecules* **2002**, *35*, 5517–5528.
- [29] S. K. Goswami, L. R. Hanton, C. J. McAdam, S. C. Moratti, J. Simpson, *Acta Crystallogr. Sect. E* **2014**, *70*, 130–133.
- [30] G. N. Ramachandran, A. V. Lakshminarayanan, *Proc. Natl. Acad. Sci. USA* **1971**, *68*, 2236–2240.
- [31] F. J. M. Hoebe, P. Jonkheijm, E. W. Meijer, A. Schenning, *Chem. Rev.* **2005**, *105*, 1491–1546.
- [32] a) G. W. Scherer, D. M. Smith, D. Stein, *J. Non-Cryst. Solids* **1995**, *186*, 309–315; b) G. W. Scherer, D. M. Smith, X. Qiu, J. M. Anderson, *J. Non-Cryst. Solids* **1995**, *186*, 316–320; c) G. Reichenauer, *Part. Part. Syst. Charact.* **2004**, *21*, 117–127.

Received: March 29, 2015

Published online: July 16, 2015